

**Quorum Sensing**
How to cite: *Angew. Chem. Int. Ed.* **2022**, *61*, e202201798

International Edition: doi.org/10.1002/anie.202201798

German Edition: doi.org/10.1002/ange.202201798

# Sustained Release of a Synthetic Autoinducing Peptide Mimetic Blocks Bacterial Communication and Virulence *In Vivo*

Korbin H. J. West, Curran G. Gahan, Patricia R. Kierski, Diego F. Calderon, Ke Zhao, Charles J. Czuprynski,\* Jonathan F. McAnulty,\* David M. Lynn,\* and Helen E. Blackwell\*

**Abstract:** There is significant interest in approaches to the treatment of bacterial infections that block virulence without creating selective pressures that lead to resistance. Here, we report the development of an “anti-virulence” strategy that exploits the activity of potent synthetic inhibitors of quorum sensing (QS) in *Staphylococcus aureus*. We identify peptide-based inhibitors of QS that are resistant to sequestration or degradation by components of murine tissue and demonstrate that encapsulation of a lead inhibitor in degradable polymer microparticles provides materials that substantially inhibit QS *in vitro*. Using a murine abscess model, we show that this inhibitor attenuates methicillin-resistant *S. aureus* (MRSA) skin infections *in vivo*, and that sustained release of the inhibitor from microparticles significantly improved outcomes compared to mice that received a single-dose bolus. Our results present an effective and modular approach to controlling bacterial virulence *in vivo* and could advance the development of new strategies for skin infection control.

## Introduction

Hospital-acquired infections present a sustained and increasingly critical health threat. *Staphylococcus aureus*, an opportunistic Gram-positive pathogen, currently causes over 100 000 hospital-acquired infections per year in the US alone, with nearly 20 000 of those infections becoming fatal.<sup>[1]</sup> A major barrier to combating *S. aureus* infections is the emergence of widespread resistance to conventional antibiotics, with strains such as the persistent methicillin-resistant *S. aureus* (MRSA) plaguing healthcare systems worldwide.<sup>[2]</sup> This emerging antibiotic crisis has motivated researchers to explore alternative, non-biocidal approaches to treat and clear bacterial infections. So-called “anti-virulence” strategies are of particular interest in this context, as they aim to reduce the severity of an infection without killing the infective organism. By doing so, they reduce selective pressures that ultimately lead to resistance and potentially allow a host’s immune response to naturally clear the infection.<sup>[3]</sup>

Quorum sensing (QS) is a cell–cell communication system used by bacteria that relies on the production and reception of chemical signals.<sup>[4]</sup> Because many human pathogens use QS to regulate the production of virulence factors that lead to or further sustain infections, QS presents an attractive target for the development of new anti-virulence approaches.<sup>[4,5]</sup> QS in *S. aureus* and other related Gram-positive bacteria is governed by the accessory gene regulator (*agr*) QS system, which utilizes an autoinducing peptide (AIP) as its signalling molecule. The *agr* system is now widely understood to be a major regulator of virulence in *S. aureus*, controlling biofilm formation and the production of hemolysins and toxic shock syndrome toxin, among many other virulence factors.<sup>[6]</sup> In recent years, chemical inhibition of the *agr* system has proven effective in attenuating *S. aureus* virulence phenotypes in bacterial cultures.<sup>[7]</sup> Several reports have demonstrated that *agr*-based QS can be strongly antagonized by a range of synthetic small-molecules,<sup>[7b,d,8]</sup> natural products (or their derivatives),<sup>[9]</sup> and macromolecular agents.<sup>[10]</sup> To date, peptide-based *agr* inhibitors represent the most potent and efficacious QS blockers known in *S. aureus*.<sup>[6b,7a,e,11]</sup>

The ability of certain *agr* inhibitors to attenuate *S. aureus* infections *in vivo* has been investigated in past studies using murine models. As an example, co-injection of non-cognate native AIPs with *S. aureus* has been reported to inhibit *agr* activity in a skin abscess model by competing with the cognate AIP during infection, preventing *agr* activation and

[\*] K. H. J. West, K. Zhao, D. M. Lynn, H. E. Blackwell  
 Department of Chemistry, University of Wisconsin-Madison  
 1101 University Ave., Madison, WI 53706 (USA)  
 E-mail: blackwell@chem.wisc.edu

C. G. Gahan, D. M. Lynn  
 Department of Chemical and Biological Engineering, University of Wisconsin-Madison  
 1415 Engineering Dr., Madison, WI 53706 (USA)  
 E-mail: dlynn@engr.wisc.edu

P. R. Kierski, J. F. McAnulty  
 Department of Surgical Sciences, School of Veterinary Medicine,  
 University of Wisconsin-Madison  
 2015 Linden Dr., Madison, WI 53706 (USA)  
 E-mail: jonathan.mcanulty@wisc.edu

D. F. Calderon, C. J. Czuprynski  
 Department of Pathobiological Sciences, School of Veterinary  
 Medicine, University of Wisconsin-Madison  
 2015 Linden Dr., Madison, WI 53706 (USA)  
 E-mail: charles.czuprynski@wisc.edu

© 2022 The Authors. Angewandte Chemie International Edition published by Wiley-VCH GmbH. This is an open access article under the terms of the Creative Commons Attribution Non-Commercial NoDerivs License, which permits use and distribution in any medium, provided the original work is properly cited, the use is non-commercial and no modifications or adaptations are made.

thereby reducing abscess formation.<sup>[12]</sup> These results are exciting in view of the well characterized cross-activity between many *agr* systems and non-cognate AIPs.<sup>[6c,7e,13]</sup> However, native AIPs have short half-lives *in vivo* ( $\approx 4$  hours)<sup>[12a]</sup> and are susceptible to interference with or sequestration by host proteins.<sup>[10a,b,14]</sup> Small-molecule<sup>[7b,8]</sup> and natural product-based<sup>[9a-c]</sup> *agr* inhibitors can also attenuate *S. aureus* infection *in vivo*; however, the lower potencies of these agents often necessitate larger quantities of compound to be administered (e.g., on the order of micrograms per animal), and the mechanisms by which some of these inhibitors function are not yet well understood.<sup>[9a,b]</sup>

Many important questions remain to be answered before inhibition of the *agr* system can be deployed *in vivo* as an effective anti-virulence strategy. For example, while inhibition of *agr* can block the production of toxins and exo-products that are part of acute *S. aureus* infections,<sup>[7a,15]</sup> many studies have shown that inhibition/deletion of *agr* and its downstream targets can promote biofilm formation *in vitro*<sup>[16]</sup> and indeed many clinical isolates of chronic infections are *agr*-deficient.<sup>[17]</sup> However, *in vivo* studies also suggest that reduced *agr* activity (or that of its downstream targets) appears to slow bacterial dissemination to other organs.<sup>[18]</sup> There are few studies that explicitly investigate how chemical inhibition of *agr* affects *in vivo* biofilm formation<sup>[17a]</sup> and a recent report has challenged the established inverse relationship between *agr* activity and biofilm *in vivo*,<sup>[19]</sup> suggesting further studies are needed to better understand the complex interplay of *agr* modulation and biofilm formation *in vivo*. In addition, many of the most potent synthetic QS modulators are thioester-linked peptide macrocycles<sup>[7a,e,11a]</sup> that, like their native AIP counterparts, can have short half-lives, low solubilities in biologically-relevant media, and are prone to sequestration or degradation by serum proteins.<sup>[10a,b,14]</sup> New agents and delivery strategies are needed to examine *S. aureus* QS more systematically *in vivo*.

In this study, we report the identification of a stable and exceptionally potent synthetic peptide-based inhibitor of the *agr* system that attenuates *S. aureus* skin infections in a murine dermonecrosis abscess model. We first identified synthetic QS inhibitors that are resistant to interference by host tissue sequestration and degradation using an initial *ex vivo* screen, and then investigated the ability of a lead compound to attenuate skin infections caused by a group-I MRSA strain *in vivo*. Our results demonstrate that this QS inhibitor can substantially reduce the severity of infection in this abscess model, and that delivery of this inhibitor using degradable polymers can prolong release and significantly improve infection outcomes relative to mice receiving a single bolus administration of the inhibitor. The results of this proof-of-concept study present an effective and potentially modular anti-virulence approach to controlling *S. aureus* skin infections *in vivo* in a mouse wound model. In a broader context, this work also provides new and useful chemical/material tools that could be used to address fundamental connections between QS and *S. aureus* infection. With further development, this research effort could

provide a pathway toward new approaches that target QS as a therapeutic strategy.

## Results and Discussion

We began our studies by focusing on a set of six synthetic peptide-based inhibitors of the *S. aureus agr* system on which we reported previously (Figure 1).<sup>[7a,21]</sup> This family of inhibitors comprises thioester- and amide-containing full or tail-truncated (tr) structural mimics of native AIP signals used by *S. aureus*, all of which are highly potent and efficacious at blocking *agr* activity, as measured in cell-based reporter gene assays and QS phenotypic assays (i.e., hemolysin and other toxin production). Most of these compounds are highly active inhibitors across all four *S. aureus agr* specificity groups (I–IV)<sup>[7a,21a,22]</sup> and none exhibit growth inhibitory effects on *S. aureus* in culture at concentrations up to at least 10  $\mu\text{M}$ .

A series of exploratory experiments with one of our most potent inhibitors (AIP-III D4A; Figure 1) showed only a limited benefit to wound healing in a murine open-wound model of *S. aureus* infection, even at relatively high concentrations (e.g., at 10  $\mu\text{M}$ ;  $>20000$ -fold above the  $\text{IC}_{50}$  of this compound in culture).<sup>[7a]</sup> We considered the possibility that this outcome could result from inactivation of this inhibitor *in vivo*. Prior reports revealed native AIPs to be relatively short-lived *in vivo* (as highlighted above),<sup>[12a]</sup> likely due to sequestration by proteins in serum (e.g., apolipoprotein B; ApoB)<sup>[10a,b,14]</sup> or other proteins that can degrade native AIP signals. We therefore developed an *ex vivo* assay (Figure S1) to evaluate this inhibitor in the presence of murine tissue samples ( $\approx 6$  mm in diameter; 1 mm thick; acquired via a tissue punch of C57BL/6-type mouse epidermis; see Methods). AIP-III D4A was incubated in the presence of tissue punches at 4.85  $\mu\text{M}$  (10000-fold above its  $\text{IC}_{50}$ ) in PBS for 24 hours. Portions of the supernatant were removed over time, diluted 100-fold, and added to a group-I *S. aureus agr* fluorescence reporter strain to measure inhibitor activity (see Methods). This reporter strain produces native AIP at wild-type levels, activating the *agr* system at quorate cell densities and inducing expression of yellow fluorescent protein (YFP). The level of YFP fluorescence thus serves as a proxy for *agr* activity, and the efficacy of added inhibitors can be measured by reductions in fluorescence.

We found that AIP-III D4A was no longer capable of fully inhibiting *S. aureus agr* activity (Figure 2, blue line) after 24 hours of *ex vivo* incubation with mouse tissue, even at the relatively high concentration used in this experiment ( $\approx 10000$ -fold its  $\text{IC}_{50}$ ). The roughly 25 % loss of *agr* inhibition at 24 hours corresponds to approximately 150 nM of free and active compound remaining in solution (as determined from a previous dose-response assay).<sup>[7a]</sup> This substantial reduction represents a  $\approx 95$  % loss of active compound. We have previously shown that AIPs in general are modestly stable to thioester hydrolysis in PBS ( $\approx 20$  % hydrolysis after 24 hours).<sup>[21a]</sup> A control study performed with AIP-III D4A in the absence of mouse tissue revealed

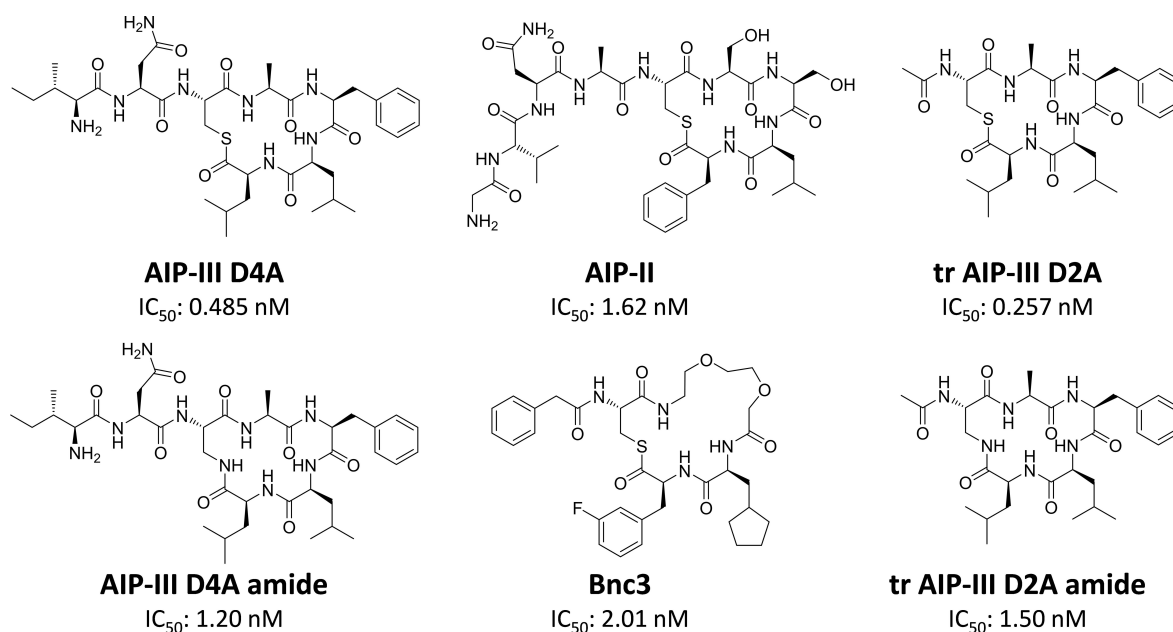


**Figure 1.** Chemical structures and potency values for QS inhibitors evaluated in this study. Potency values are from previous reports (see references [7a, 21]) and were determined by dose-dependent inhibition of compounds in cell-based *agr* reporter assays in wild-type *S. aureus* (group-I).

no loss of inhibitory activity in 24 hr (Figure S2). Taken together, these results suggest that AIP-III D4A is degraded or sequestered by components of mouse tissue. Subsequent experiments demonstrated that this loss of activity could be prevented by heat treating the tissue sample at 80 °C for 15 min prior to the addition of AIP-III D4A (Figure S3; see Methods), suggesting that the loss of activity we observe likely involves a tissue protein or other component that is rendered irreversibly non-functional by heat.

We used this *ex vivo* assay to identify synthetic inhibitors that were stable to components of murine skin tissue. The results of a screen of all six inhibitors shown in Figure 1 at concentrations 10000-fold above their respective IC<sub>50</sub> values is illustrated in Figure 2. Inspection of these results reveals several useful structure-function relationships. AIP-II (a native *S. aureus* AIP; orange curve) and Bnc3 (a synthetic

peptidomimetic based on AIP-II; black curve)<sup>[21b]</sup> lost nearly all antagonistic activity within 24 hours, far exceeding the 25 % loss in inhibitory activity observed for the synthetic AIP-III mimic, AIP-III D4A. AIP-III D4A amide (red curve),<sup>[21a]</sup> an analog of AIP-III D4A in which the thioester is replaced with a more hydrolytically-stable amide linkage, exhibited a loss of activity that was similar in magnitude to that of AIP-III D4A (blue curve). This result suggests that the loss of activity of AIP-III D4A in the experiments above was not a result of accelerated thioester hydrolysis. In stark contrast to these results, tr AIP-III D2A<sup>[7a]</sup> (green curve) and tr AIP-III D2A amide (purple curve),<sup>[21a]</sup> which are truncated (tr) versions of AIP-III D4A and AIP-III D4A amide in which the exocyclic tail is replaced with acetyl group, maintained essentially full activity after 24 hours of incubation with murine tissue.

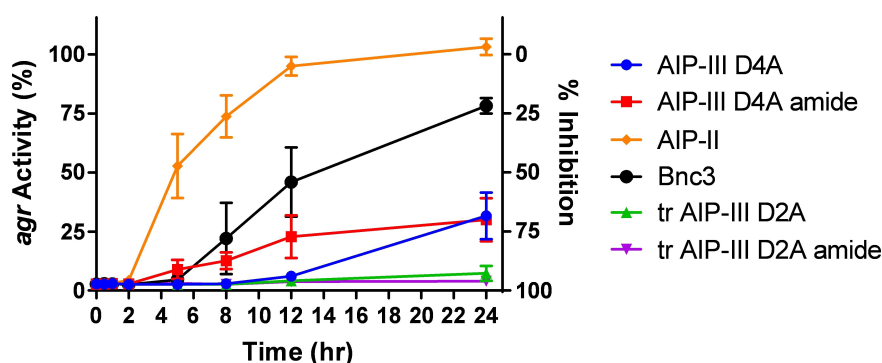


**Figure 2.** Time courses of *S. aureus agr* activity for compounds incubated with mouse tissue. *agr* activity was measured using a fluorescent reporter assay. Values shown are the average and SEM of three ( $n=3$ ) independent *ex vivo* experiments normalized to vehicle (100% activity) and media (0% activity) controls.

The reason for the markedly high retention of activity by these truncated compounds is unclear; however, we note that the absence of the two amino acid tail and the lack of a free amine terminus alter the polarity, amphipathic nature, and solution-phase conformation of these compounds,<sup>[22]</sup> which could substantially impact interactions with proteins present in skin tissue. Additional experiments in which AIP-III D4A and tr AIP-III D2A were incubated with ApoB—an apolipoprotein commonly found in skin and blood<sup>[23]</sup> that has been reported to bind to and sequester AIPs<sup>[10a,b]</sup>—provided additional support for this view. When we incubated AIP-III D4A with ApoB for three hours, we observed a substantial and statistically significant decrease in AIP-III D4A recovered by analytical HPLC compared to controls lacking ApoB (Figure S4A,C). In contrast, we observed essentially no loss of tr AIP-III D2A when it was incubated with ApoB under identical conditions (Figure S4B,D). Additional experiments will be required to understand more fully the basis for the increased stability and activity of these truncated compounds, and we note that our identification of ApoB interactions as a possible mechanism for ligand inactivation does not exclude other pathways. In the context of the current study, however, this *ex vivo* screen identified two surprisingly stable and potent candidates for further evaluation *in vivo*. We selected tr AIP-III D2A (mol. wt. 589.75 g mol<sup>-1</sup>) for use in all subsequent *in vivo* studies described below based on its high potency in culture against group-I *S. aureus* (IC<sub>50</sub> = 0.257 nM; Figure 1) and the observation that, as noted above, it has no influence on growth at high concentrations in culture (up to 50 μM; Figure S5).

We next evaluated the ability of tr AIP-III D2A to attenuate *S. aureus* infection using a murine dermonecrosis abscess model.<sup>[24]</sup> This model and related acute skin infection models have been used in past studies to characterize the role of *agr* activity in *S. aureus* infections, including both genetic approaches with *agr* mutant strains<sup>[7b,c,9b]</sup> and chemical approaches involving co-injection with non-cognate native AIPs<sup>[7c,12]</sup> or small-molecule QS inhibitors.<sup>[7b,9a,b]</sup> In this model, lesion development is evaluated over time by imaging the animals on predetermined days and measuring the areas of visible lesions. To validate this model in our hands, we first compared abscess formation in mice inoculated with a common group-I *S. aureus* strain or with a mutant ( $\Delta agr$ ) lacking a functional *agr* system (see Methods). We observed significantly larger abscesses to develop in mice inoculated with the wild-type strain than in mice inoculated with the  $\Delta agr$  strain (Figure S6). This result is comparable to previous reports indicating that  $\Delta agr$  mutants are attenuated with regard to acute skin infection.<sup>[7b,c,9b,12a]</sup>

We then co-injected 2.5 nmol of tr AIP-III D2A (1.5 μg; 50 μM [ $\approx 195\,000 \times IC_{50}$ ] at the time of injection) or a vehicle control solution (DMSO with no inhibitor) with a 50 μL culture of USA300 LAC MRSA and monitored infection over the course of a week using the murine abscess model. While co-injection of bacteria with compound does not mimic a clinical scenario, it provides confidence in this controlled study that the bacteria are exposed to a sufficient concentration of compound to elicit its inhibitory effect and

allows for comparison to past studies using this same mouse model. The total molar amount of tr AIP-III D2A injected in these experiments had no negative effects on *S. aureus* growth *in vitro* (Figure S5) and was comparable to or less than those used to evaluate other QS inhibitors *in vivo* in past studies.<sup>[7b,c,9b]</sup> tr AIP-III D2A had no observed gross toxicity or effect on mouse body weight using this model over the course of the experiment (Figure S7A).

Lesions were imaged 1, 3, 5, and 7 days after inoculation, and representative images of mice in treated groups and untreated vehicle control groups are shown in Figure 3A. Treatment with tr AIP-III D2A significantly reduced the sizes of lesions on each day relative to vehicle controls (Figure 3B), with only half of the inhibitor-treated mice showing visible lesions seven days after infection, as opposed to 90% of the vehicle control group (see Supporting Information for pictures of the abscesses of all mice in this study on day 7). These results indicate that bolus administration of tr AIP-III D2A can substantially diminish the severity of *S. aureus* skin infections in this mouse model. These results constitute the first demonstration of inhibitory activity *in vivo* using this class of synthetic *agr* inhibitors based on native AIP-III and are consistent with *agr* inhibition as the likely cause for attenuation.

We conducted additional experiments to investigate the ability of tr AIP-III D2A to inhibit *S. aureus* skin infections in this mouse model when loaded into degradable polymer microparticles. For these studies, we adapted a previously reported electrospaying protocol<sup>[25]</sup> to fabricate pseudo-spherical microparticles of PLG (lactide:glycolide (50:50); 30–60 kDa; see Methods), with diameters of 1.48 ( $\pm 0.38$ ) μm (as characterized by SEM; see Figure 4A and Figure S8) that were sized appropriately to fit through the 25 gauge needles used in our *in vivo* experiments. These microparticles were measured to contain 1.22 ( $\pm 0.17$ ) nmol of peptide/mg polymer as determined using analytical HPLC (see Methods and Figure S9), or approximately 21% of the maximum theoretical loading of peptide using this fabrication approach. These particles released approximately 22 pmol of tr AIP-III D2A per mg of particle into solution over 21 days when incubated in PBS, with a large burst release over the first 24 hours (Figure 4B; as determined using a biological reporter assay; see Methods, Equations S1 and S2, Figure S10, and the Supporting Information for additional information related to these experiments). We estimate this amount to correspond to less than 1% of the total loaded peptide, suggesting that these particle formulations could be used to promote release over much longer time periods than those evaluated here.

Characterization of released inhibitor using our *S. aureus* fluorescent *agr* reporter strain revealed that (i) tr AIP-III D2A retained its biological activity upon release from PLG and (ii) sufficient amounts were released for each of the first four days to fully inhibit *agr* activity. Amounts released in each subsequent 24-hour time period did not completely inhibit *agr* activity, but substantial inhibition was observed out to day 7 under the conditions evaluated here (Figure 4C, D, Figure S11). We note that it should be straightforward to further modify and optimize the loading and release profiles



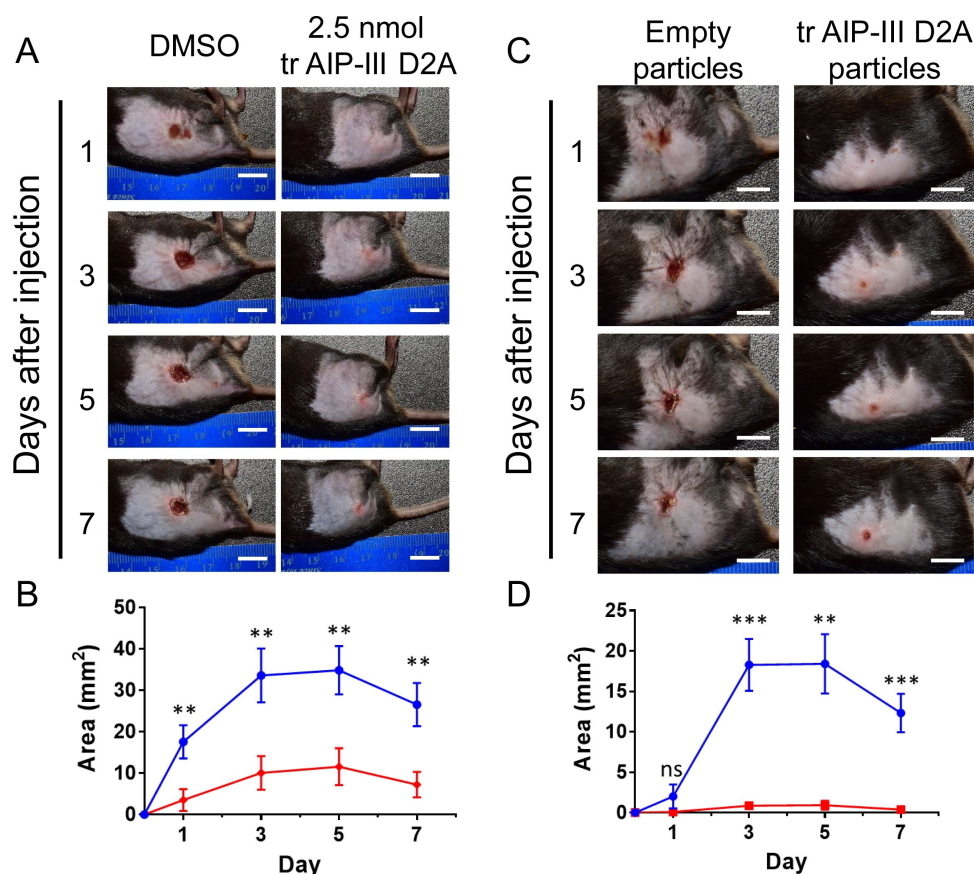


**Figure 3.** Abscess attenuation due to tr AIP-III D2A delivered as a 2.5 nmol bolus in solution (A), (B) or delivered in 1 mg of PLG microparticles (C), (D). A) Representative images for the DMSO vehicle and compound-treated groups. B) Average abscess size with SEM for vehicle group (blue line,  $n=10$ ) and compound-treated group (red line,  $n=10$ ). C) Representative images for groups treated with empty, non-loaded microparticles and compound-loaded microparticles. D) Average abscess size with SEM for empty microparticle group (blue line,  $n=9$ ) and compound-loaded microparticle group (red line,  $n=10$ ). Statistical analysis with Mann–Whitney test,  $**p < 0.01$ ,  $***p < 0.001$ . Scale bars represent 1 cm.

of these particles by adjusting the chemical and physical properties of PLG and/or process parameters used to fabricate the particles.<sup>[26]</sup> That said, the sizes, loadings, and *in vitro* release profiles of the particles reported here were sufficient for all subsequent proof-of-concept experiments in mice described below.

We next examined whether controlled release of tr AIP-III D2A could replicate or surpass the efficacy of bolus administration for attenuating *S. aureus* skin infection *in vivo*. Guided by the results of the *in vitro* release experiments above, we selected an amount of loaded microparticles capable of releasing sufficient of tr AIP-III D2A to block *agr* activity over a one-week period. Using the mouse abscess model, we co-injected 50  $\mu$ L of USA300 LAC MRSA culture and either i) 1 mg of tr AIP-III D2A-loaded microparticles (1.22 nmol [720 ng] of inhibitor in total) or ii) 1 mg of unloaded (no inhibitor) microparticles into mice. Representative images from these experiments are shown in Figure 3C. We observed lesions that were significantly smaller for the inhibitor-loaded particle group, as compared to the empty particle group on every day other than day 1 (Figure 3D). Comparing the final abscess sizes on day 7, only a single mouse out of 10 from the inhibitor-loaded

particle-treated group had an observable lesion (2.89 mm<sup>2</sup>). In contrast, nearly 80 % of the mice in the control group (no inhibitor) had lesions with an average size of 15.8 mm<sup>2</sup> (see Supporting Information for images of the abscesses of all mice in this study on day 7). We conclude on the basis of these results that the polymer microparticles release tr AIP-III D2A in a form that remains biologically active *in vivo*, and that this controlled release strategy yields a concentration profile at the site of infection over a seven-day period that is sufficient to inhibit bacterial virulence at levels comparable to, if not better than, those observed in the single-dose, bolus administration *in vivo* experiments described above.

The results shown in Figure 3 not only demonstrate that tr AIP-III D2A can provide significant protection against acute *S. aureus* skin infection, but also suggest that well-understood advantages of strategies for the localized and controlled release of active agents used in other scenarios<sup>[27]</sup> can provide additional practical benefits in this context. Specifically, we note that the amount of compound released over the course of 7 days in the microparticle-treated mice in the experiments above, if it were to occur at a rate similar to that of the *in vitro* release profile in Figure 4B, would be

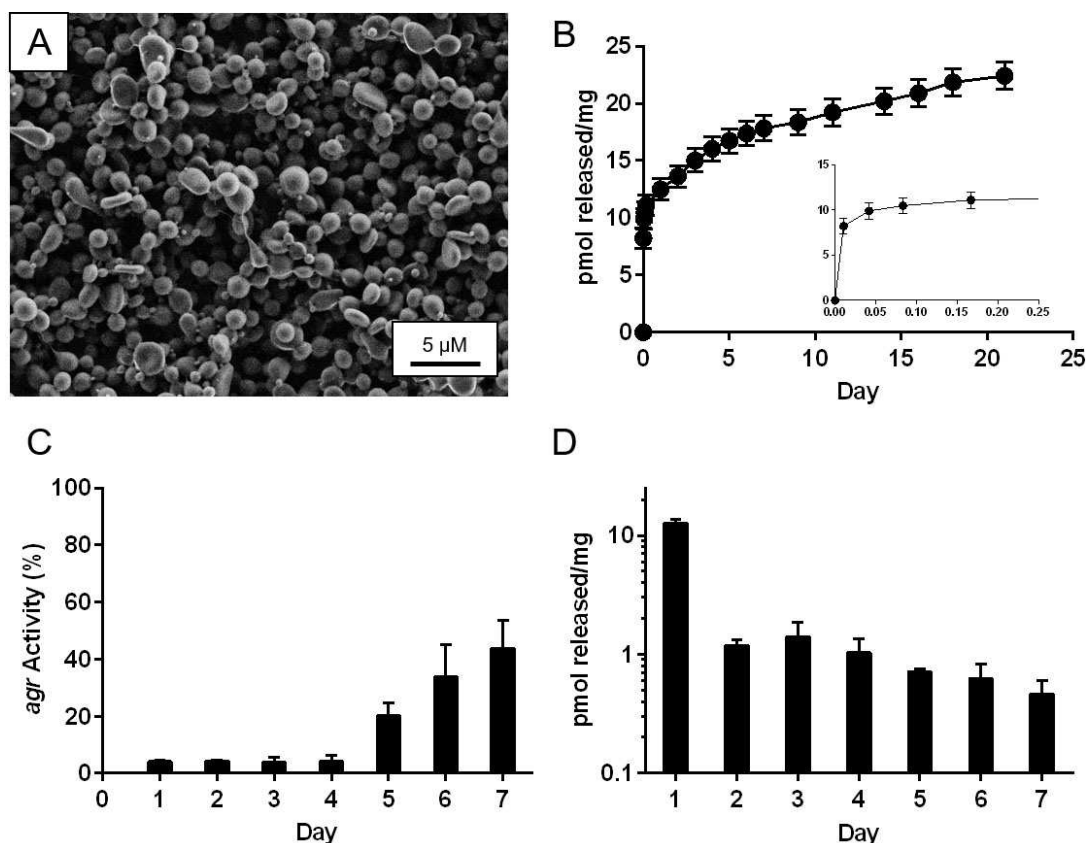


**Figure 4.** Characterization of PLG microparticles loaded with tr AIP-III D2A. A) Top-down SEM images of tr AIP-III D2A-loaded PLG microparticles fabricated by electrospraying. B) The normalized cumulative release of tr AIP-III D2A from the PLG microparticles over three weeks. C) The *agr* activity of the *S. aureus* reporter incubated with undiluted aliquots acquired each day from the release experiments. D) The normalized release of tr AIP-III D2A from the PLG microparticles each day. The values shown in (B)–(D) are the average and single standard deviation for three ( $n = 3$ ) independent release experiments.

approximately 18 pmol, which is nearly 100-fold less than the amount that was administered in the single-dose, bolus administration experiment (2.5 nmol). We are aware that the rate of release of tr AIP-III D2A *in vivo* could be different from that which we observed *in vitro*. In view of the complexities of the abscess environment, we were unable to accurately determine the release profiles of our loaded particles *in vivo*. We note further, however, that irrespective of potential differences in the rates of controlled release *in vivo*, the results of our *in vivo* experiments with these microparticles are consistent with the gradual release of tr AIP-III D2A, the subsequent inhibition of *S. aureus* virulence *in vivo* through a mechanism that involves *agr* inhibition, and the known benefits of controlled release for bioactive agents.

We performed a final series of *in vivo* experiments to obtain a side-by-side comparison of the efficacies of a single-dose, bolus administration of tr AIP-III D2A to treatment with the tr AIP-III D2A-loaded microparticles when the total amounts of inhibitor available at the infection site were comparable. Using the mouse abscess model, we compared the efficacy of 1 mg of inhibitor-loaded microparticles (an amount that, again, released 18 pmol of tr AIP-III D2A over 7 days in our *in vitro* experiments) directly to a similar

amount of inhibitor (25 pmol) administered as a single-dose, bolus injection. As shown in Figure 5, this single bolus dose of tr AIP-III D2A did not attenuate *S. aureus* infection at any time point as compared to control mice ( $p > 0.05$ ; Kruskal–Wallis test). In contrast, the tr AIP-III D2A-loaded microparticle treatment substantially reduced abscess size at each time point ( $p < 0.05$  for day 5,  $p < 0.01$  for days 1, 3, and 7; Kruskal–Wallis test), consistent with the results of the previous microparticle experiments above (Figure 3C, D). This result strongly underscores potential benefits arising from the sustained release of inhibitor in preventing abscess formation by *S. aureus* and is further consistent with the well-established ability of controlled release approaches to substantially improve therapeutic outcomes at reduced loadings of active agent.<sup>[27]</sup> We attribute the superior performance of the controlled release formulation to its ability to sustain effective locally high concentrations of inhibitor in the immediate vicinity of the infection site. Conversely, the bolus administration of soluble inhibitor can rapidly drain or diffuse away from the injection site, reducing the local concentration of inhibitor below what is needed to reduce the severity of infection.

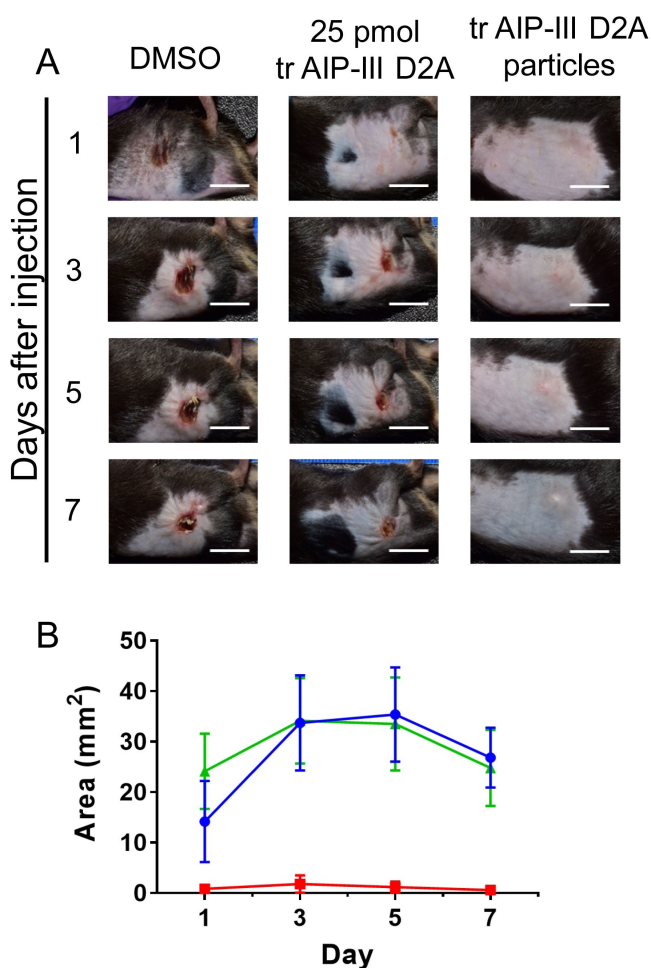


**Figure 5.** Side-by-side comparison of abscess formation after treatment with tr AIP-III D2A in solution vs. PLG microparticles. A) Representative images from mice treated with vehicle, a solution of compound, or compound loaded in microparticles. B) Average abscess size with SEM of mice treated with vehicle (green,  $n=8$ ), 25 pmol of tr AIP-III D2A in solution (blue line,  $n=8$ ), or with 1 mg of microparticles (red line,  $n=8$ ). Data analyzed with Kruskal–Wallis test. Scale bars represent 1 cm.

## Conclusion

Our results demonstrate i) the ability of a potent synthetic peptide inhibitor of *S. aureus* QS to attenuate bacterial virulence *in vivo* using an acute skin infection model and ii) an efficacious controlled release strategy for reducing *S. aureus* infection using this anti-virulence approach. These results were enabled by the preliminary *ex vivo* screening of *S. aureus* *agr*-inhibitors to identify compounds resistant to inactivation by components present in mouse tissue. We identified a lead inhibitor, tr AIP-III D2A, that nearly completely blocks MRSA skin infection in a mouse dermonecrosis abscess model following a single-dose bolus administration, or by injection of polymer microparticles that sustain the local release of the inhibitor at the infection site. Our results demonstrate significantly greater efficacy using the polymer microparticles versus the single-dose approach, underscoring the potential strategic value of using

sustained-release strategies for the administration of QS inhibitors and development of new anti-virulence approaches to combat bacterial skin infections.

The results of this study are important for several reasons. First, we demonstrate the ability of a lead *agr* inhibitor—one of the most potent known inhibitors of *S. aureus* QS in culture—to strongly block *S. aureus* infection in an *in vivo* mouse model of skin infection. Second, our results reveal tail truncation of two AIP-derived mimetics to be an effective strategy to eliminate interference by host tissue, in sharp contrast to the observed inactivation of similar native AIPs and their close analogs in the presence of tissue. This observation underpins, at least in part, the efficacy and potency of tr AIP-III D2A *in vivo* and provides guidance that will prove useful for the design and discovery of new inhibitors suitable for use *in vivo*. Third, our results demonstrate that controlled release strategies can improve the therapeutic potential of these truncated inhibitors and reduce to nanograms the total amount of compound required to attenuate infection *in vivo*. Notably, these findings represent more than an order of magnitude improvement compared to previous *in vivo* studies that required the administration of microgram quantities of less-potent *agr* inhibitors for efficacy in similar skin infection models.<sup>[7b,9a–c,12a]</sup> Past studies have investigated strategies for the encapsulation of bacterial QS inhibitors into materials and the testing of these approaches *in vitro* and *ex vivo*.<sup>[28]</sup> The results of this current study represent, to our knowledge, the first report of the successful application of a controlled release QS inhibition strategy to abate *S. aureus* infection *in vivo*.

More broadly, the discovery of stable and highly potent inhibitors and the identification of strategies that enable controlled release and local availability of this class of agents during infection provide powerful tools, alone or in combination, to address a range of important fundamental questions. These include the role of *agr* QS in long-term chronic infections and biofilm formation,<sup>[16c,17a,19]</sup> and the emergence of spontaneous QS mutants commonly isolated from patients with such infections.<sup>[3a,15,29]</sup> These tools also provide a foundation for the development of new types of materials (e.g., surface coatings) that could effectively attenuate bacterial virulence in or around implantable or indwelling medical devices, or on other commercial surfaces on which *S. aureus* colonization and infections are endemic. Looking beyond *S. aureus*, the approach reported here should also be readily applicable to other combinations of QS inhibitors, QS activators, and polymers, significantly expanding the utility of chemical methods to explore and modulate QS pathways and outcomes, and thus has implications for new therapeutic interventions.

**Supporting Information:** Full experimental methods, additional cell-based, *ex vivo* and *in vivo* assay data, microparticle characterization, and final time point images from dermonecrosis model experiments.



## Acknowledgements

Financial support for this work was provided by the NIH (R21 AI135745), the Wisconsin Alumni Research Foundation (WARF) UW2020 Program, and the NSF through a grant provided to the UW-Madison Materials Research Science and Engineering Center (MRSEC; DMR-1720415). The authors acknowledge the use of instrumentation supported by the NSF through the UW MRSEC (DMR-1720415). K.H.J.W. was supported in part by the UW-Madison NIH Chemistry-Biology Interface Training Program (T32GM008505). C.G.G. was supported in part by a NSF Graduate Research Fellowship. J.F.M. and C.J.C. acknowledge the Walter and Martha Renk Endowed Laboratory for Food Safety and the UW-Madison Food Research Institute. We thank Prof. Alexander Horswill (University of Colorado Medical School) for *S. aureus* strains and Prof. Tom Turng (UW-Madison) for providing access to electrospraying instrumentation, and acknowledge support for those facilities provided by the Wisconsin Institutes of Discovery and the Vice Chancellor for Research and Graduate Education at UW-Madison.

## Conflict of Interest

The authors declare no conflict of interest.

## Data Availability Statement

The data that support the findings of this study are available from the corresponding author upon reasonable request.

**Keywords:** Anti-Infective · Cell–Cell Signalling · Controlled Release · Peptides · Quorum Sensing

- [1] A. P. Kourtis, K. Hatfield, J. Baggs, Y. Mu, I. See, E. Epton, J. Nadle, M. A. Kainer, G. Dumyati, S. Petit, S. M. Ray, Emerging Infections Program MRSA author group, D. Ham, C. Capers, H. Ewing, N. Coffin, L. C. McDonald, J. Jernigan, D. Cardo, *Morb. Mortal. Wkly. Rep.* **2019**, *68*, 214–219.
- [2] a) S. Y. Tong, J. S. Davis, E. Eichenberger, T. L. Holland, V. G. Fowler, Jr., *Clin. Microbiol. Rev.* **2015**, *28*, 603–661; b) M. Z. David, R. S. Daum, *Clin. Microbiol. Rev.* **2010**, *23*, 616–687; c) E. Klein, D. L. Smith, R. Laxminarayan, *Emerging Infect. Dis.* **2007**, *13*, 1840–1846.
- [3] a) C. A. Ford, I. M. Hurford, J. E. Cassat, *Front. Microbiol.* **2020**, *11*, 632706; b) S. W. Dickey, G. Y. C. Cheung, M. Otto, *Nat. Rev. Drug Discovery* **2017**, *16*, 457–471; c) R. C. Allen, R. Popat, S. P. Diggle, S. P. Brown, *Nat. Rev. Microbiol.* **2014**, *12*, 300–308.
- [4] M. Whiteley, S. P. Diggle, E. P. Greenberg, *Nature* **2017**, *551*, 313–320.
- [5] a) S. Azimi, A. D. Klementiev, M. Whiteley, S. P. Diggle, *Annu. Rev. Microbiol.* **2020**, *74*, 201–219; b) B. LaSarre, M. J. Federle, *Microbiol. Mol. Biol. Rev.* **2013**, *77*, 73–111.
- [6] a) R. P. Novick, E. Geisinger, *Annu. Rev. Genet.* **2008**, *42*, 541–564; b) B. Wang, T. W. Muir, *Cell Chem. Biol.* **2016**, *23*, 214–224; c) M. Thoendel, J. S. Kavanaugh, C. E. Flack, A. R. Horswill, *Chem. Rev.* **2011**, *111*, 117–151.
- [7] a) Y. Tal-Gan, D. M. Stacy, M. K. Foegen, D. W. Koenig, H. E. Blackwell, *J. Am. Chem. Soc.* **2013**, *135*, 7869–7882; b) E. K. Sully, N. Malachowa, B. O. Elmore, S. M. Alexander, J. K. Femling, B. M. Gray, F. R. DeLeo, M. Otto, A. L. Cheung, B. S. Edwards, L. A. Sklar, A. R. Horswill, P. R. Hall, H. D. Gresham, *PLoS Pathog.* **2014**, *10*, e1004174; c) P. Mayville, G. Ji, R. Beavis, H. Yang, M. Goger, R. P. Novick, T. W. Muir, *Proc. Natl. Acad. Sci. USA* **1999**, *96*, 1218–1223; d) A. M. Salam, C. L. Quave, *mSphere* **2018**, *3*, e00500–00517; e) A. R. Horswill, C. P. Gordon, *J. Med. Chem.* **2020**, *63*, 2705–2730.
- [8] D. Kuo, G. Yu, W. Hoch, D. Gabay, L. Long, M. Ghannoum, N. Nagy, C. V. Harding, R. Viswanathan, M. Shoham, *Antimicrob. Agents Chemother.* **2015**, *59*, 1512–1518.
- [9] a) D. A. Todd, C. P. Parlet, H. A. Crosby, C. L. Malone, K. P. Heilmann, A. R. Horswill, N. B. Cech, *Antimicrob. Agents Chemother.* **2017**, *61*, e00263–00217; b) C. P. Parlet, J. S. Kavanaugh, H. A. Crosby, H. A. Raja, T. El-Elimat, D. A. Todd, C. J. Pearce, N. B. Cech, N. H. Oberlies, A. R. Horswill, *Cell Rep.* **2019**, *27*, 187–198.e186; c) S. M. Daly, B. O. Elmore, J. S. Kavanaugh, K. D. Triplett, M. Figueroa, H. A. Raja, T. El-Elimat, H. A. Crosby, J. K. Femling, N. B. Cech, A. R. Horswill, N. H. Oberlies, P. R. Hall, *Antimicrob. Agents Chemother.* **2015**, *59*, 2223–2235; d) A. Nielsen, M. Mansson, M. S. Bojer, L. Gram, T. O. Larsen, R. P. Novick, D. Frees, H. Frokiaer, H. Ingmer, *PLoS One* **2014**, *9*, e84992; e) J. Brango-Vanegas, L. A. Martinho, L. J. Bessa, A. G. Vasconcelos, A. Placido, A. L. Pereira, J. Leite, A. H. L. Machado, *Beilstein J. Org. Chem.* **2019**, *15*, 2544–2551; f) P. Piewngam, Y. Zheng, T. H. Nguyen, S. W. Dickey, H. S. Joo, A. E. Villaruz, K. A. Glose, E. L. Fisher, R. L. Hunt, B. Li, J. Chiou, S. Pharkjaksu, S. Khongthong, G. Y. C. Cheung, P. Kiratisin, M. Otto, *Nature* **2018**, *562*, 532–537.
- [10] a) M. M. Peterson, J. L. Mack, P. R. Hall, A. A. Alsup, S. M. Alexander, E. K. Sully, Y. S. Sawires, A. L. Cheung, M. Otto, H. D. Gresham, *Cell Host Microbe* **2008**, *4*, 555–566; b) B. O. Elmore, K. D. Triplett, P. R. Hall, *PLoS One* **2015**, *10*, e0125027; c) F. Da, L. Yao, Z. Su, Z. Hou, Z. Li, X. Xue, J. Meng, X. Luo, *J. Appl. Microbiol.* **2017**, *122*, 257–267.
- [11] a) G. J. Lyon, J. S. Wright, T. W. Muir, R. P. Novick, *Biochemistry* **2002**, *41*, 10095–10104; b) Q. Xie, M. M. Wiedmann, A. Zhao, I. R. Pagan, R. P. Novick, H. Suga, T. W. Muir, *Chem. Commun.* **2020**, *56*, 11223–11226.
- [12] a) J. S. Wright III, R. Jin, R. P. Novick, *Proc. Natl. Acad. Sci. USA* **2005**, *102*, 1691–1696; b) M. M. Brown, J. M. Kwiecinski, L. M. Cruz, A. Shahbandi, D. A. Todd, N. B. Cech, A. R. Horswill, *Antimicrob. Agents Chemother.* **2020**, *64*, e00172–00120.
- [13] G. Ji, R. Beavis, R. P. Novick, *Science* **1997**, *276*, 2027–2030.
- [14] J. M. Yarwood, J. K. McCormick, M. L. Paustian, V. Kapur, P. M. Schlievert, *J. Bacteriol.* **2002**, *184*, 1095–1101.
- [15] G. Y. C. Cheung, J. S. Bae, M. Otto, *Virulence* **2021**, *12*, 547–569.
- [16] a) C. Vuong, C. Gerke, G. A. Somerville, E. R. Fischer, M. Otto, *J. Infect. Dis.* **2003**, *188*, 706–718; b) C. Vuong, H. L. Saenz, F. Gotz, M. Otto, *J. Infect. Dis.* **2000**, *182*, 1688–1693; c) B. R. Boles, A. R. Horswill, *PLoS Pathog.* **2008**, *4*, e1000052.
- [17] a) C. Vuong, S. Kocianova, Y. Yao, A. B. Carmody, M. Otto, *J. Infect. Dis.* **2004**, *190*, 1498–1505; b) C. M. Suligoy, S. M. Lattar, M. Noto Llana, C. D. Gonzalez, L. P. Alvarez, D. A. Robinson, M. I. Gomez, F. R. Buzzola, D. O. Sordelli, *Front. Cell. Infect. Microbiol.* **2018**, *8*, 18.
- [18] a) S. Periasamy, H. S. Joo, A. C. Duong, T. H. Bach, V. Y. Tan, S. S. Chatterjee, G. Y. Cheung, M. Otto, *Proc. Natl. Acad. Sci. USA* **2012**, *109*, 1281–1286; b) R. Wang, B. A. Khan, G. Y.



- Cheung, T. H. Bach, M. Jameson-Lee, K. F. Kong, S. Y. Queck, M. Otto, *J. Clin. Invest.* **2011**, *121*, 238–248.
- [19] S. C. Jordan, P. R. Hall, S. M. Daly, *Sci. Rep.* **2022**, *12*, 1251.
- [20] a) K. Schilcher, A. R. Horswill, *Microbiol. Mol. Biol. Rev.* **2020**, *84*, e00026-19; b) K. Y. Le, S. Dastgheyb, T. V. Ho, M. Otto, *Front. Cell. Infect. Microbiol.* **2014**, *4*, 167.
- [21] a) Y. Tal-Gan, M. Ivancic, G. Cornilescu, T. Yang, H. E. Blackwell, *Angew. Chem. Int. Ed.* **2016**, *55*, 8913–8917; *Angew. Chem.* **2016**, *128*, 9059–9063; b) J. K. Vasquez, H. E. Blackwell, *ACS Infect. Dis.* **2019**, *5*, 484–492.
- [22] Y. Tal-Gan, M. Ivancic, G. Cornilescu, C. C. Cornilescu, H. E. Blackwell, *J. Am. Chem. Soc.* **2013**, *135*, 18436–18444.
- [23] a) M. Mommaas, J. Tada, M. Ponec, *J. Dermatol. Sci.* **1991**, *2*, 97–105; b) K. R. Feingold, P. M. Elias, M. Mao-Qiang, M. Fartasch, S. H. Zhang, N. Maeda, *J. Invest. Dermatol.* **1995**, *104*, 246–250.
- [24] C. Bunce, L. Wheeler, G. Reed, J. Musser, N. Barg, *Infect. Immun.* **1992**, *60*, 2636–2640.
- [25] B. Almería, W. Deng, T. M. Fahmy, A. Gomez, *J. Colloid Interface Sci.* **2010**, *343*, 125–133.
- [26] a) J. M. Anderson, M. S. Shive, *Adv. Drug Delivery Rev.* **1997**, *28*, 5–24; b) H. K. Makadia, S. J. Siegel, *Polymers* **2011**, *3*, 1377–1397; c) K. E. Uhrich, S. M. Cannizzaro, R. S. Langer, K. M. Shakesheff, *Chem. Rev.* **1999**, *99*, 3181–3198; d) M. A. Tracy, K. L. Ward, L. Firouzabadian, Y. Wang, N. Dong, R. Qian, Y. Zhang, *Biomaterials* **1999**, *20*, 1057–1062.
- [27] a) S. Mitragotri, P. A. Burke, R. Langer, *Nat. Rev. Drug Discovery* **2014**, *13*, 655–672; b) M. W. Tibbitt, J. E. Dahlman, R. Langer, *J. Am. Chem. Soc.* **2016**, *138*, 704–717; c) O. S. Fenton, K. N. Olafson, P. S. Pillai, M. J. Mitchell, R. Langer, *Adv. Mater.* **2018**, *30*, 1705328.
- [28] a) M. J. Kratochvil, T. Yang, H. E. Blackwell, D. M. Lynn, *ACS Infect. Dis.* **2017**, *3*, 271–280; b) M. J. Kratochvil, Y. Tal-Gan, T. Yang, H. E. Blackwell, D. M. Lynn, *ACS Biomater. Sci. Eng.* **2015**, *1*, 1039–1049; c) A. H. Broderick, D. M. Stacy, Y. Tal-Gan, M. J. Kratochvil, H. E. Blackwell, D. M. Lynn, *Adv. Healthcare Mater.* **2014**, *3*, 97–105; d) A. H. Broderick, A. S. Breitbach, R. Frei, H. E. Blackwell, D. M. Lynn, *Adv. Healthcare Mater.* **2013**, *2*, 993–1000; e) N. Singh, M. Romero, A. Travanut, P. F. Monteiro, E. Jordana-Lluch, K. R. Hardie, P. Williams, M. R. Alexander, C. Alexander, *Biomater. Sci.* **2019**, *7*, 4099–4111; f) H. D. Lu, A. C. Spiegel, A. Hurley, L. J. Perez, K. Maisel, L. M. Ensign, J. Hanes, B. L. Bassler, M. F. Semmelhack, R. K. Prud'homme, *Nano Lett.* **2015**, *15*, 2235–2241; g) N. Nafee, A. Husari, C. K. Maurer, C. Lu, C. de Rossi, A. Steinbach, R. W. Hartmann, C. M. Lehr, M. Schneider, *J. Controlled Release* **2014**, *192*, 131–140.
- [29] K. E. Traber, E. Lee, S. Benson, R. Corrigan, M. Cantera, B. Shopsin, R. P. Novick, *Microbiology* **2008**, *154*, 2265–2274.

Manuscript received: February 2, 2022

Accepted manuscript online: March 25, 2022

Version of record online: April 12, 2022